

Antimode dynamics and chaotic itinerancy in the coherence collapse of semiconductor lasers with optical feedback

Takuya Sano*

NTT Transmission Systems Laboratories, 1-2356 Take, Yokosuka, Kanagawa 238-03, Japan

(Received 9 December 1993)

Low-frequency fluctuations observed in the coherence collapse of semiconductor lasers are numerically investigated based on the Lang-Kobayashi model. It is found that the attractor in the compound cavity mode loses its stability due to a crisis with an antimode. Chaotic itinerancy among the destabilized compound cavity modes is also found.

PACS number(s): 42.50.Ne, 42.55.Px, 42.60.Mi, 05.45.+b

I. INTRODUCTION

Semiconductor lasers with delayed optical feedback show a variety of behaviors because the delay configuration intrinsically creates an infinite number of degrees of freedom. This rich variety of behavior has been attracting many researchers' attention from both the scientific and the practical points of view. Scientists believed that this system was a good candidate for exploring low-dimensional chaos. Along this line, two possible routes to deterministic chaos were found: the period-doubling route [1] and the quasiperiodic route [2]. For practical applications, on the other hand, this rich dynamical behavior can cause problems that must be overcome. For instance, either weak or strong feedback can realize single-mode narrow-linewidth operation, while moderate feedback causes the linewidth to increase dramatically up to several tens of gigahertz. This drastic linewidth broadening is called coherence collapse [3]. The coherence-collapse state has been studied in terms of deterministic chaos by several authors [4–6]. At moderate feedback levels, intermittent drops in light intensity, each followed by a gradual increase, have been observed near the lasing threshold [7] and, in the frequency domain, these drops manifest themselves as low-frequency fluctuations (LFF) [7,8] at frequencies less than one-tenth the external cavity resonance frequency. These drops cause a kink in the light-current characteristic. Several authors claim that this phenomenon is noise-induced switching between bistable states. Henry and Kazarinov introduced a potential model considering that the maximum-gain-reduction mode is always linearly stable but because of the higher-order term the potential well has a peak that can be surmounted by spontaneous emission noise [9]. Their approximate analytical results well explained the qualitative current dependency of the drop period. This conjecture was further pursued by Mørk, Tromborg, and Christiansen [10]. Their theoretical analysis suggests that these drops are noise-induced switching from the stable maximum-gain-reduction mode

to the temporally stable (within the external cavity round-trip time) minimum-linewidth mode. They demonstrated numerical simulations that included the noise effect and reproduced the repetitive drops. They performed other simulations that omitted the spontaneous emission noise and were able to reproduce at least one deterministic drop. This possible deterministic drop suggests that the conjecture of noise-induced switching might be valid only for the initial switching from the originally stable state (the maximum-gain-reduction mode) and not for the subsequent drop process. The actual mechanism of the drop is not yet known. Research to date, however, has been based on either the adiabatic elimination technique, by which only the initial transition from the stable state could be analyzed [11], or incomplete direct analysis. It is necessary to analyze the model equations directly in terms of nonlinear dynamics.

This paper investigates the origin of the intensity drops based on the Lang-Kobayashi equations. In Sec. II, we derive the steady-state solutions of the equations, some of which correspond to the known compound cavity modes and the others correspond to antimodes, which are always unstable saddle-type solutions. We plot the location of these solutions in phase space. The next section introduces the direct numerical calculations of the Lang-Kobayashi equations that reproduce the deterministic intensity drop phenomenon. The dependency of this phenomenon on variations in injection current is also demonstrated to duplicate the characteristics found in previous experimental results. In the fourth section, the numerical solutions are compared with the steady-state solutions in phase space. It is found that each intensity drop is initiated by crisis: a collision with an unstable saddle solution. Moreover, we find chaotic itinerancy [12,13] observed as switching between destabilized compound cavity modes. A simple example of how the crisis is reached is shown in the fifth section. The sixth section introduces a physical interpretation.

II. MODEL EQUATIONS AND STATIONARY SOLUTIONS

This paper assumes that even in the regime of relatively strong feedback and near the lasing threshold, the

*FAX: 81-468-55-1285; electronic address: tsano@ntttd.nnt.jp

Lang-Kobayashi equations are a good representation of the physical process. Here, we concentrate on the physics of the drop phenomenon, so we use the normalized equations [14]

$$\frac{dP}{dt} = \Delta NP + 2\gamma\sqrt{P(t-\tau)P(t)} \cos[\phi(t) - \phi(t-\tau) + \omega\tau] + \beta N + F_P(t), \quad (1)$$

$$\frac{d\phi}{dt} = \frac{\alpha}{2} \Delta N - \gamma \left[\frac{P(t-\tau)}{P(t)} \right]^{1/2} \times \sin[\phi(t) - \phi(t-\tau) + \omega\tau] + F_\phi(t), \quad (2)$$

$$\frac{d\Delta N}{dt} = -\Delta N - (K + \Delta N)P + \Delta J + F_{\Delta N}(t). \quad (3)$$

These are the temporal evolution equations for the photon number P , the slowly varying part of the optical phase ϕ , and the deviation of the carrier number from the threshold value N_{th} of the solitary laser $\Delta N \equiv N - N_{\text{th}}$. In this notation, ω stands for the optical angular frequency of the solitary laser, K is the damping constant for the photon number, and ΔJ is the pumping-current deviation from the threshold of the solitary laser. α is the linewidth enhancement factor and τ is the round-trip time of the external cavity. The feedback strength γ is given by

$$\gamma = \eta \frac{(1-r)}{\tau_c} \left[\frac{R}{r} \right]^{1/2}, \quad (4)$$

where R is the power reflectivity of the external mirror, r is that of the laser facets, τ_c is the round-trip time of the laser cavity, and η is the coupling ratio. $F_P(t)$, $F_\phi(t)$, and $F_{\Delta N}(t)$ are Langevin noise terms representing stochastic spontaneous emission events and β is the spontaneous emission factor. These equations have succeeded in explaining weak feedback effects both for Fabry-Pérot lasers and for distributed-feedback lasers. This paper neglects stochasticity, which blocks the investigation of the fully deterministic problem, and sets some of the parameters to typical values: $\alpha=6$, $\beta=10^{-5}$, $K=10^3$, $\eta=1$, and $N_{\text{th}}=10^3$.

For simplicity, we omit the term representing the contribution of the spontaneous emission to the photon-number evolution in (1), i.e., $\beta=0$, so the stationary solutions are easily obtained as

$$\Delta N = -2\gamma \cos\varphi, \quad (5)$$

$$P = \frac{\Delta J + 2\gamma \cos\varphi}{K - 2\gamma \cos\varphi}, \quad (6)$$

$$\Delta\omega\tau = -\alpha\gamma\tau \cos\varphi + \gamma\tau \sin\varphi = -\gamma\tau\sqrt{1+\alpha^2} \sin(\varphi + \arctan\alpha), \quad (7)$$

where $\varphi \equiv \phi(t) - \phi(t-\tau) + \omega\tau$ is the phase difference between the field inside the laser cavity and the field fed back into the cavity. The determination of ϕ from Eq. (7) is only possible numerically since (7) is a transcendental equation. The solutions of (7) can be graphically obtained as shown in Fig. 1. Since the value of $\gamma\tau$ deter-

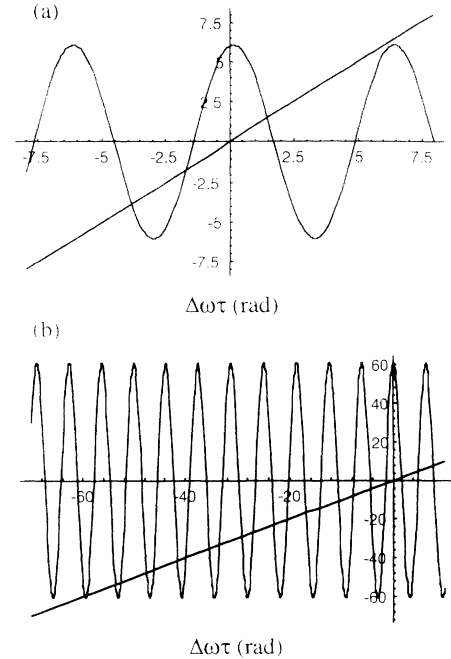


FIG. 1. Graphical solutions of the equations. (a) $\gamma=1$, $\tau=1$; (b) $\gamma=1$, $\tau=10$.

mines the amplitudes of the sine term of (7), the number of solutions increases as the value increases. For this reason, several authors used $\gamma\tau$ as a control parameter to discriminate the operation region [15]. A linear stability analysis suggests that there are two types of solutions; one type is always unstable and the other is stable or unstable depending on the parameter values [16]. Following the definition given in Ref. [2], the former is called the antimode, and the latter is the usual compound cavity mode (eigenmode). Both types of solutions are created in pairs by a saddle-node bifurcation [2].

From (4) and (6), the steady-state solutions lie on an ellipse, as illustrated in Fig. 2, as was shown by Henry and Kazarinov [9],

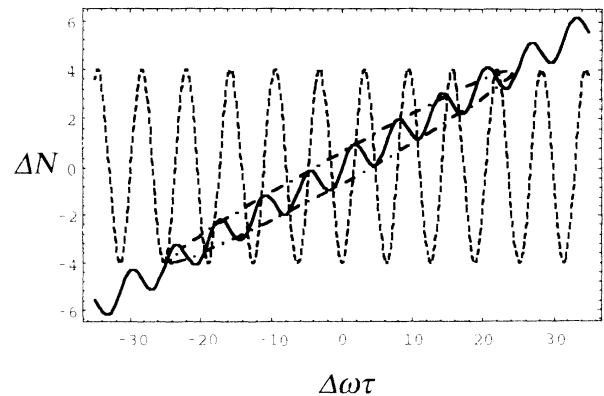


FIG. 2. Steady-state solutions in the ΔN - $\Delta\omega\tau$ space. The solid line is the phase condition curve, and the dashed line is the gain condition curve. The intersections of these curves fall on an ellipse (dash-dotted line).

$$\left[\Delta\omega\tau - \frac{\alpha\tau}{2}\Delta N \right]^2 + \left[\frac{\tau}{2}\Delta N \right]^2 = (\gamma\tau)^2. \quad (8)$$

The compound cavity modes are located in the lower half of the ellipse, whereas the antimodes lie on the upper half. The detuning value $\omega\tau$ simply changes the location of these solutions in a clockwise direction along the ellipse circumference. The solution at the lowest point of this ellipse corresponds to the mode with the lowest gain, where $\varphi \approx 2\pi n$ (n is an integer) and $\Delta N \approx -2\gamma$, and the solution with $\varphi \approx 2\pi n - \arctan\alpha$ and $\Delta N \approx 0$ corresponds to the mode with minimum linewidth, which is located at the center [17]. At the strong and distant feedback limit ($\gamma\tau \sim \infty$), the number of solutions increases, resulting in more solutions on the ellipse. If we restrict φ in the range between 0 and 2π , then there exists a solution for any φ regardless of the detuning value $\omega\tau$. This fact allows us to neglect the $\omega\tau$ dependence of the solutions at the large- $\gamma\tau$ limit. The following analysis assumes $\omega\tau = 0$.

III. NUMERICAL SIMULATIONS

The equations are solved directly using the Runge-Kutta method. Here, we consider the case of relatively strong feedback (power reflection rate $\approx 1\%$) and distant reflection (the delay time much larger than the carrier lifetime). Figure 3 shows calculated temporal wave forms for $\gamma = 5$ and $\tau = 20$. Figure 3(a) shows the temporal evolution of the photon number with smoothing, considering the limited bandwidth of the measurement setup usually employed. The figure clearly demonstrates that the deterministic intensity drops are followed by gradual steplike increases, with each step equivalent to the round-trip time. Figures 3(b) and 3(c) depict the corresponding temporal evolution of the carrier number ΔN and the phase difference $\phi(t) - \phi(t - \tau)$, respectively. We can also see the sudden rise in the carrier-number plot even without smoothing, and the sudden change of the phase relation in the phase-difference plot. The dependency of the drop period on pumping current is shown in Fig. 4. In this figure, only the carrier numbers are plotted. The drop period shortens as the pumping level increases, paralleling the widely known observed dependence [5,7,8].

Here, we can no longer resort to the potential model introduced by Henry and Kazarinov [9] to explain this dependence, since their model assumes a stable fixed-point solution and a finite amount of spontaneous emission noise.

To gain insight into the main features of the dynamics, the simple case of a small $\gamma\tau$ value ($\gamma = 5$, $\tau = 2$) is calculated and plotted in Fig. 5. The temporal evolution of the phase difference [Fig. 5(a)] more clearly suggests switching between destabilized compound cavity modes (quasi-attractor) since the lifetimes of all modes are longer than in the previous example. In the case of carrier number [Fig. 5(b)], large oscillation conceals only small switching events, not those corresponding to the intensity drops. To characterize this phenomenon more precisely, the cal-

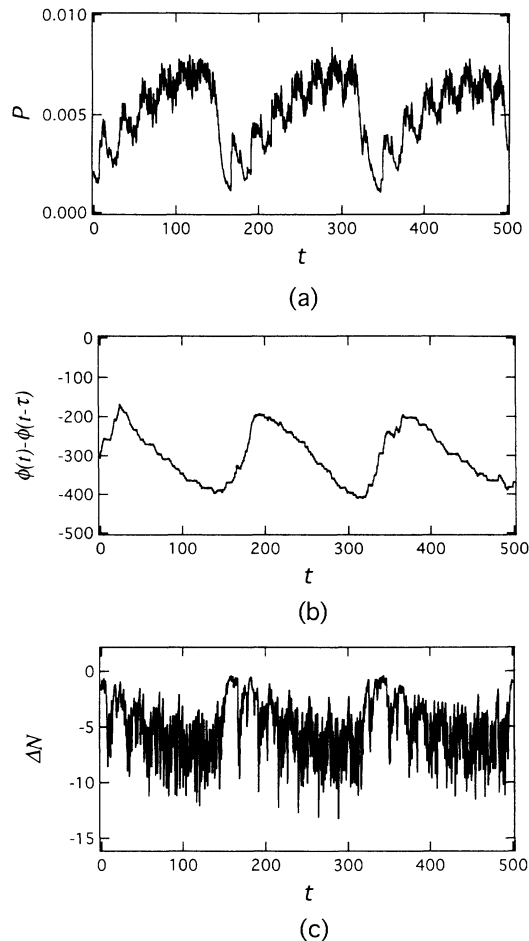


FIG. 3. Calculated temporal wave forms for (a) the smoothed photon number P , (b) phase difference $\phi(t) - \phi(t - \tau)$, and (c) the carrier number ΔN . The parameters are $\gamma = 5$, $\tau = 20$, and $\Delta J = 0.00$.

culated points are plotted onto the phase space mentioned in the previous section to yield Fig. 5(c). According to this figure, the buildup process is due to the change in lasing mode, driven by oscillation in the carrier number, from smaller phase-difference modes to larger phase-difference modes (right to left). The drop process, on the other hand, occurs in the antimode region (the upper half of the ellipse). The phase-space plot also indicates that each drop is initiated by a collision between the quasiattractor in one of the compound cavity modes and the associated antimode. This collision is what we call a crisis in nonlinear dynamics [18]. After the crisis, the carrier number ΔN increases almost directly to the threshold value 0, and then the phase difference shifts to a smaller value, which is almost equivalent to the threshold value of the solitary laser.

It should also be pointed out that switching to higher frequencies, opposite to the normal buildup direction can occur randomly during the buildup process. We call this kind of switching *inverse switching* (IS) and regard it as a sign of chaotic itinerancy [12,13]. Chaotic itinerancy is

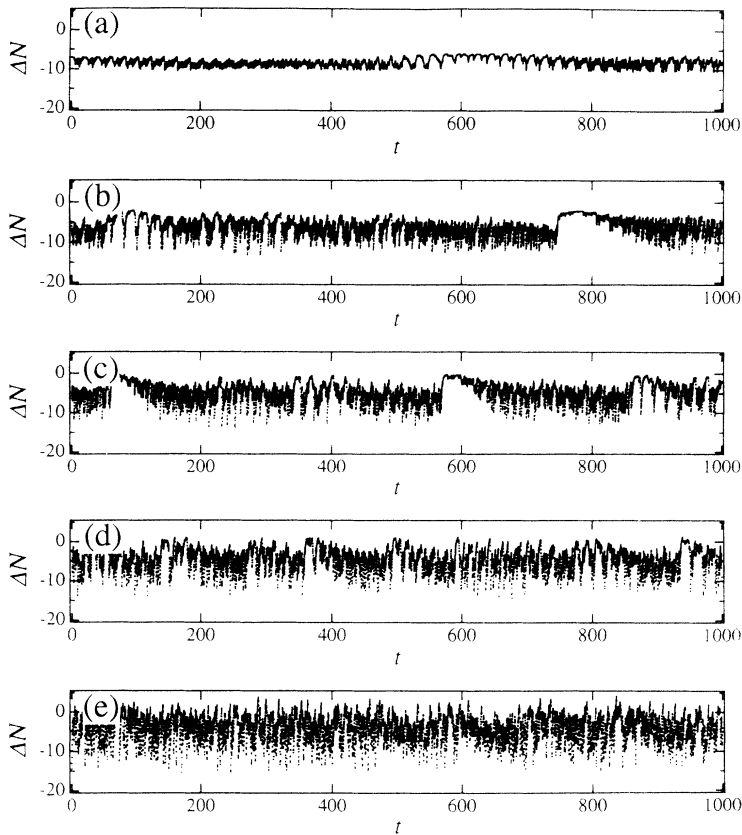


FIG. 4. Change of the wave form of the carrier number ΔN with variation in the pumping current J . (a) $\Delta J = -6.0$, (b) $\Delta J = -2.0$, (c) $\Delta J = 0.0$, (d) $\Delta J = 2.0$, and (e) $\Delta J = 6.0$.

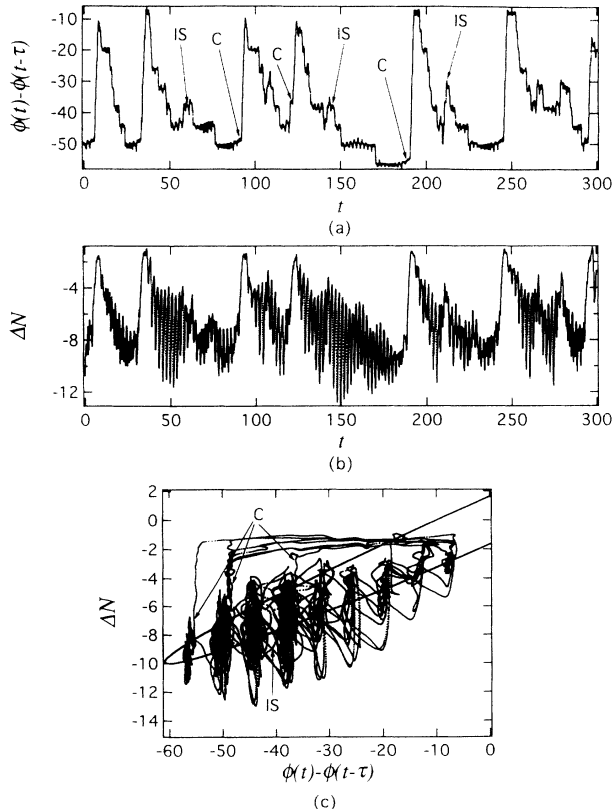


FIG. 5. Simulated wave forms of the phase difference $\phi(t) - \phi(t - \tau)$ (a) and the carrier number ΔN (b) and their phase-space portrait (c) for $\gamma = 5$ and $\tau = 2$. Crisis and inverse switching are denoted by C and IS, respectively.

deterministic random switching between quasiattractors, and is widely seen in dynamical systems with high degrees of freedom. In the present case, the compound cavity modes which lose stability correspond to the quasiattractors, and the trajectory moves from one of these to another during the buildup process. Although switching mainly occurs in one direction, from smaller to larger phase-difference modes, this motion is randomly interrupted by switching in the other direction. The interesting point is that the high degrees of freedom of this system originate from the feedback delay, not the number of variables themselves.

IV. EXAMPLE OF CRISIS

In this section, the process that leads to a crisis is described precisely as the change of an attractor through parameter variations. To this end, we choose a certain compound cavity mode solution as an initial condition and observe how the attractor changes. We take $\beta = 0$ in order to simplify the choice of the initial condition. The injection current is the control parameter, and is increased from slightly above the modified lasing threshold. Figure 6 shows changes in the attractor against six injection currents at the mode of the minimum carrier number using the condition specified for Fig. 5, and Fig. 7 shows the corresponding fast Fourier transform (FFT) power spectra.

When $\Delta J = -9.7$, the attractor is a fixed point, i.e., the laser operates in the stable compound cavity mode. For $\Delta J = -9.0$, the attractor is a periodic limit cycle, which

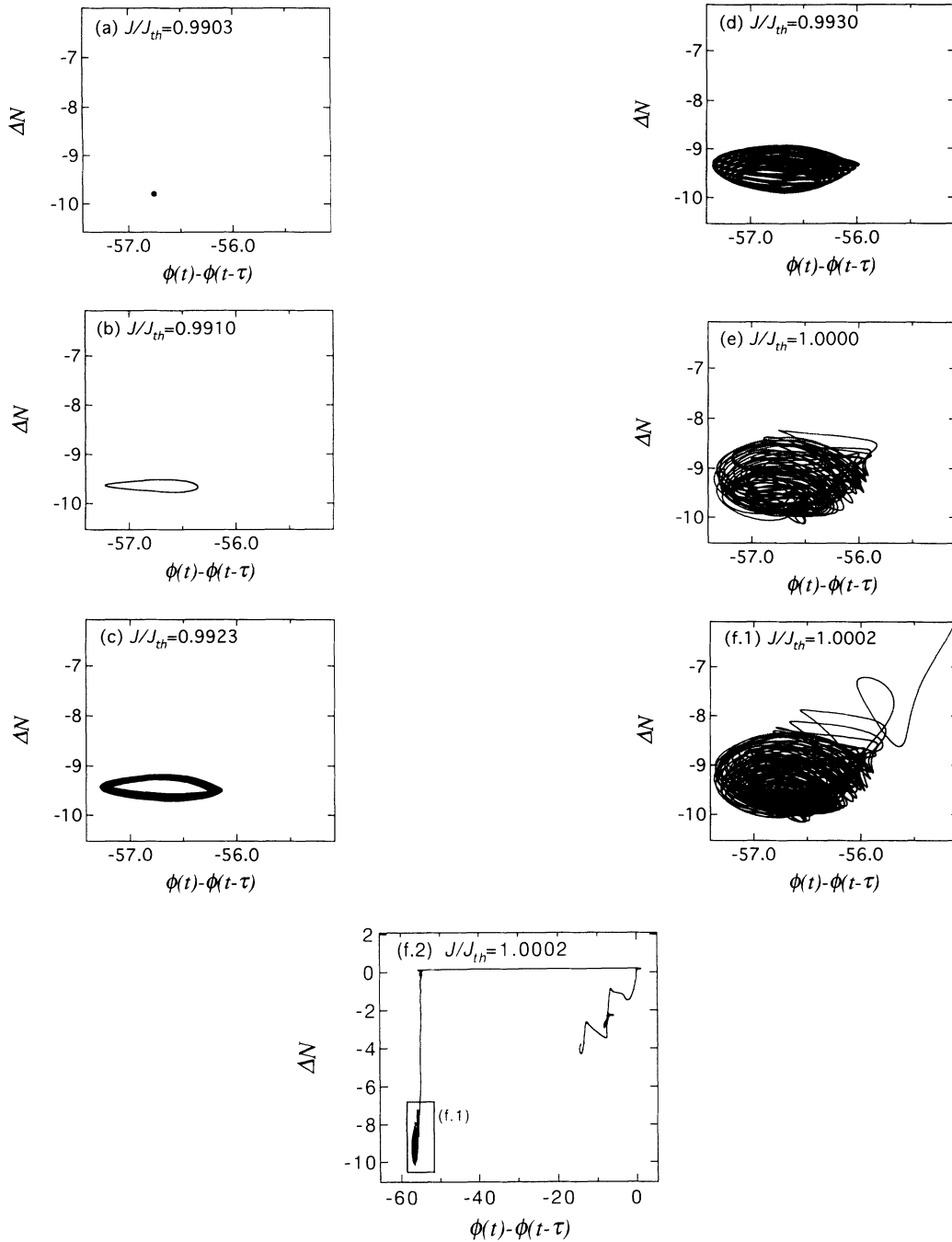


FIG. 6. Change of the attractor in the compound cavity mode with increasing pumping current J . (a) A fixed-point attractor, (b) a limit cycle, (c),(d) a quasiperiodic torus, (e) a chaotic attractor, (f.1) a blowup of the attractor (crisis), and (f.2) the whole picture of (f.1) (only the transients are shown).

emerges from the fixed point due to a Hopf bifurcation. In the power spectrum, peaks are located near the inverse of the round-trip time of the external cavity and its harmonics. At $\Delta J = -7.7$, a quasiperiodic torus becomes an attractor as a result of the second Hopf bifurcation, and another peak appears in the lower-frequency region, showing the appearance of relaxation oscillation. The torus has a very complicated appearance with many exit-

ed harmonics of the lower-frequency peak, as can be seen at $\Delta J = -7.0$. At $\Delta J = 0.0$, the phase-space plot suggests the emergence of a local chaotic attractor. This is confirmed by the broad noise spectrum seen in Fig. 7(d). This is a quasiperiodic route to chaos, the same type as that found by Mørk, Tromborg, and Mark in the same system with high injection current [2]. The slight increase of injection current to $\Delta J = 0.2$ causes a crisis at

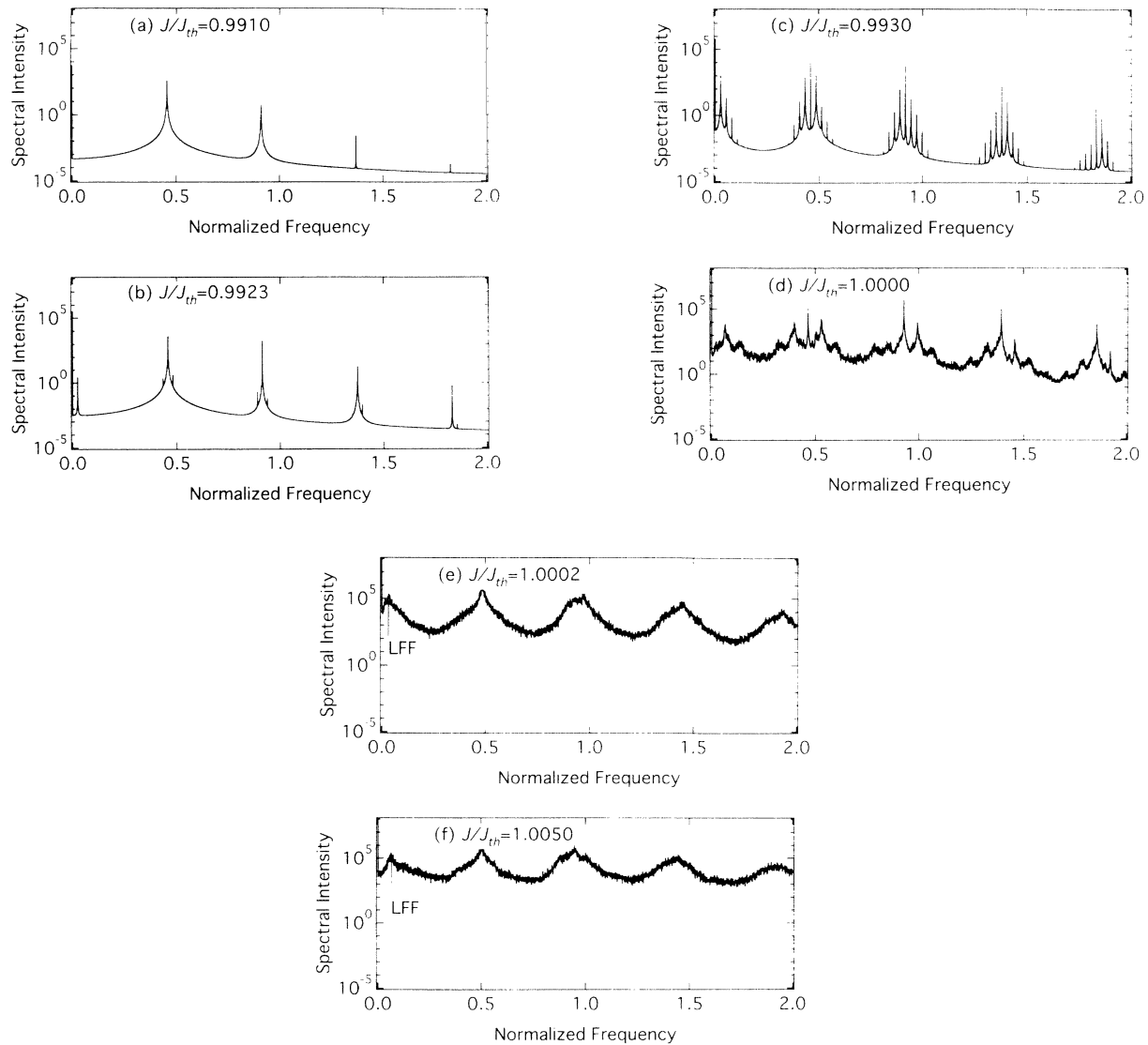


FIG. 7. Change of the power spectrum of the photon number P with increases in the pumping current J corresponding to (b), (c), (d), (e), and (f) of Fig. 6, respectively. (f) is for a slightly higher pumping current ($\Delta J = 5.0$) than (e). In (f) and (e), the low-frequency fluctuations are marked by arrows at the normalized frequency 0.031 and 0.064, respectively.

the antimode. This crisis changes the local chaotic attractor to transient chaos, equivalent to a quasiattractor. The trajectory confined in the compound cavity mode in the case of lower injection current, after some transient time, escapes away from this region toward the upper right corner of Fig. 6(f.1). The trajectory then goes straight to the threshold value of the carrier number and begins to travel a wider region of the phase space as we saw in Fig. 6(f.2) and the previous section. The corresponding power spectrum in Fig. 7(e) shows more broadening compared to the simple chaotic case of Fig. 7(d). Further increase of the injection current makes the LFF peak shift to a higher frequency from 0.031 (normalized frequency) in Fig. 7(e) to 0.064 in Fig. 7(f), which parallels other experimental results [19,20].

Figure 8 schematically illustrates this crisis. An an-

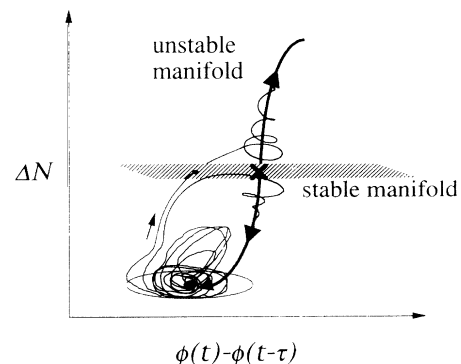


FIG. 8. Schematic illustration of the antimode dynamics (crisis).

timode is a saddle-type solution that has one stable and one unstable manifold. In this case, the stable manifold is a plane almost perpendicular to the $\Delta N - \{\phi(t) - \phi(t - \tau)\}$ plane. The unstable manifold encompasses both increases and decreases in the carrier number. A trajectory that fails to pass through the stable manifold rapidly returns to the chaotic compound cavity mode. A trajectory that passes through the stable manifold continues to head in the direction of increasing carrier number up to the threshold of the carrier number. As is suggested by Fig. 2, the antimode is also a phase-locked solution in which locking is enhanced by the strong-feedback photons compared to the decreasing photons inside the cavity, even though the refractive index changes with the photon number. As a result, the phase difference remains almost unchanged during the intensity drop, as is seen in Fig. 5.

V. DISCUSSIONS

The LFF process demonstrated so far is summarized in Fig. 9. It consists of two parts; one is the intensity buildup along the compound cavity modes and the other is the intensity drop due to crisis. The buildup process is physically interpreted as a wave-mixing process. Chaotic oscillation in a single compound cavity mode generates side modes at the other compound cavity mode frequencies, resulting in multimode oscillation. The energy in each mode is then transferred to the lower-frequency side as a result of the anomalous interaction of lasing modes as proposed by Bogatov, Eliseev, and Sverdlov [21]. They found that, in the presence of two lasing modes in a laser cavity, the lower-frequency mode acquired excess gain due to the nonlinear scattering by the dynamic grating with the beat frequency of the two modes. After the repetition of this process for several round-trip periods, changes in the refractive index cause destructive interference which reduces the optical intensity. Laser oscillation then restarts at the frequency of the solitary laser. In this way, the LFF process is repeated.

Contrary to existing studies, the intensity drop is not switching between bistable states since the new state is not stable even during the interval of the round-trip time. The intensity drop is self-generated by antimode dynamics, which is usually considered to be physically meaningless. Concerning antimodes, Ref. [2] shows an example of modes and antimodes and the corresponding potential. According to that potential, the unstable manifolds of an antimode connect two adjacent compound cavity modes. This is certainly the case for weak feedback and short round-trip time. On the other hand, for stronger-feedback conditions, where more degrees of freedom can be generated, other types of unstable manifolds, such as the one described in the present paper, appear. It is very important to consider the relation between the feedback condition and the possible dimension of the attractor since this system has an inherently infinite number of degrees of freedom.

This study also suggests that the coherent interaction between the field in the cavity and the field fed back into the cavity is necessary for the drop phenomenon. As is

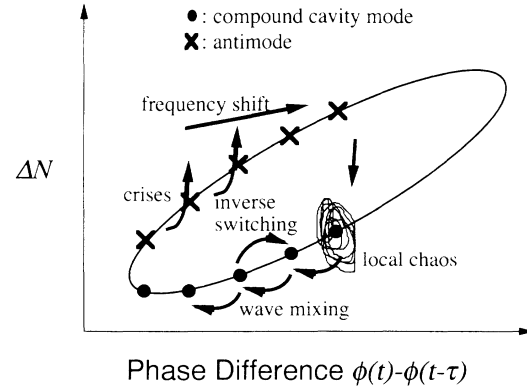


FIG. 9. Schematic illustration of the LFF process.

shown by the phase portraits, phase dynamics plays an important role even in the coherence-collapsed regime.

In this model, just one longitudinal mode is sufficient to cause the LFF process, although more degrees of freedom (the other longitudinal modes of the solitary laser and the quantum noise) seem to be necessary to simulate exact laser operations. This latter point was also mentioned by Mørk, Tromborg, and Christiansen [10]. They found that the inclusion of more longitudinal modes smoothed the LFF process and that the spontaneous emission noise also had a stabilizing effect instead of causing the drop. Despite these facts, we find that the principal dynamics is accurately modeled by the single-mode, noise-free equations.

The model equations also show chaotic itinerancy. It can be described by the chaotic modulation of the feedback effect expressed as $\gamma[P(t - \tau)/P(t)]^{1/2}$, which determines the effective locking strength. Physically, it is considered to be the result of complex interaction among the compound cavity modes and the relaxation oscillation. This paper finds that chaotic itinerancy fundamentally originates from delay, whereas research to date has considered only multiple variables.

VI. CONCLUSIONS

We investigate the dynamical properties of the Lang-Kobayashi equations near the threshold of a solitary laser. The sudden intensity drops are found to be caused by crises between local chaotic attractors and associated antimodes, which are unstable saddle-type solutions. The subsequent buildup process is shown to be switching between compound cavity mode oscillations, which is interpreted as the result of a wave-mixing process. The change in a local chaotic attractor via crisis is demonstrated. In addition, chaotic itinerancy is found during the buildup process, which is understood as the effect of complex modulation of the effective feedback rate by the relaxation oscillation.

ACKNOWLEDGMENTS

The author would like to thank K. Otsuka and K. Kikushima for helpful discussions.

- [1] T. Mukai and K. Otsuka, *Phys. Rev. Lett.* **55**, 1711 (1985).
- [2] J. Mørk, B. Tromborg, and J. Mark, *IEEE J. Quantum Electron.* **QE-28**, 93 (1992).
- [3] D. Lenstra, B. G. Verbeek, and A. J. d. Boef, *IEEE J. Quantum Electron.* **QE-21**, 674 (1985).
- [4] Y. Cho and T. Umeda, *Opt. Commun.* **59**, 131 (1986).
- [5] J. Mørk and K. Kikuchi, in *Proceedings of the Conference on Lasers and Electro-Optics '88, Anaheim, CA, 1988* (OSA, Washington, DC, 1988), p. 216.
- [6] G. C. Dente, P. S. Durkin, K. A. Wilson, and C. E. Moeller, *IEEE J. Quantum Electron.* **QE-24**, 2441 (1988).
- [7] H. Temkin, N. A. Olsson, J. H. Abeles, R. A. Logan, and M. B. Panish, *IEEE J. Quantum Electron.* **QE-22**, 286 (1986).
- [8] R. Ries and F. Sporleder, in *Proceedings of the 8th European Conference on Optical Communication, Cannes, France, 1982* (Comité de la Conférence Européenne sur les Communications Optiques, Cannes, 1982), p. 285.
- [9] C. H. Henry and R. F. Kazarinov, *IEEE J. Quantum Electron.* **QE-22**, 294 (1986).
- [10] J. Mørk, B. Tromborg, and P. L. Christiansen, *IEEE J. Quantum Electron.* **QE-24**, 123 (1988).
- [11] B. Tromborg and J. Mørk, *IEEE J. Quantum Electron.* **QE-26**, 642 (1990).
- [12] K. Ikeda, K. Otsuka, and K. Matsumoto, *Prog. Theor. Phys. Suppl.* **99**, 295 (1989).
- [13] K. Otsuka, *Phys. Rev. Lett.* **65**, 329 (1990).
- [14] R. Lang and K. Kobayashi, *IEEE J. Quantum Electron.* **QE-16**, 347 (1980).
- [15] H. Olesen, J. Henrik, and B. Tromborg, *IEEE J. Quantum Electron.* **QE-22**, 762 (1986).
- [16] B. Tromborg, J. H. Osmundsen, and H. Olesen, *IEEE J. Quantum Electron.* **QE-20**, 1023 (1984).
- [17] J. Mørk and B. Tromborg, *IEEE Photon Technol. Lett.* **2**, 21 (1990).
- [18] C. Grebogi, E. Ott, and J. A. Yorke, *Phys. Rev. Lett.* **48**, 1507 (1982).
- [19] J. O'Gorman, B. J. Hawdon, and J. Hegarty, *Electron. Lett.* **25**, 114 (1989).
- [20] M. Fujiwara, K. Kubota, and R. Lang, *Appl. Phys. Lett.* **38**, 217 (1981).
- [21] A. P. Bogatov, P. G. Eliseev, and B. N. Sverdlov, *IEEE J. Quantum Electron.* **QE-65**, 510 (1975).